PREDICTING CHANGES IN THE BEHAVIOR OF ERUPTING VOLCANOES, AND REDUCING THE UNCERTAINTIES ASSOCIATED WITH THEIR IMPACT ON SOCIETY AND THE ENVIRONMENT

Human vulnerability to volcanic eruptions is increasing, with ~500 million people living within the potential exposure range of an active volcano[1]. There are ~1500 potentially active volcanoes around the globe (Fig. 1), and a recent study[2] of 441 volcanoes in 16 developing countries revealed that 384 have little or no monitoring, including 65 volcanoes identified as posing a high risk to large populations. Although great strides have been made in terms of quantifying volcanic processes and hazards, fundamental gaps in our knowledge remain[3]. Two recent community roadmaps and reports, (Moran et al., 2008, *Instrumentation Recommendations for Volcano Monitoring at U.S. Volcanoes Under the National Volcano Early Warning System*[4] and Davis et al., 2016, *Challenges and Opportunities for Research in ESI (CORE): Report from the NASA Earth Surface and Interior (ESI) Focus Area Workshop*[5]) have identified the data and measurements required to fill these gaps. The following Science and Applications Targets (SATs) can be pursued (and significantly advanced) by means of space-based observations to satisfy these community needs, whilst substantially advancing understanding in the *Earth Surface and Interior: Dynamics and Hazards* Decadal Survey Earth System Science Theme.

SCIENCE AND APPLICATIONS TARGETS

SCIENCE TARGET: IMPROVE FORECASTS OF WHEN VOLCANIC ERUPTIONS WILL BEGIN AND END

Description of the science target, and relevance to community needs and Decadal Survey Theme

Before an eruption begins fresh magma must move to the surface, resulting in precursory seismicity, deformation, and degassing (primarily H_2O, CO_2, and SO_2)[3]. Enhanced shallow hydrothermal activity may result[6], manifesting as thermal, mineralogical and degassing anomalies at the surface. Crater lakes act as chemical condensers and calorimeters, their temperature, color and size responding to inputs of magmatic energy and elements from beneath[7]. Such changes have been observed to occur prior to eruptions[8]. Although potential precursory signals are many, a recent study of 288 cases of volcanic activity between 2000 and 2011 found that five were the primary observational indicators of volcanic unrest: ground deformation (Fig. 2), degassing (Fig. 3), changes in volcanic crater lakes (size, color and temperature; Fig. 4), surface thermal anomalies (Fig. 5), and seismicity[9]. With the exception of seismicity, all of these precursory signals can be measured from space. Sparks et al.[3] suggest that the most important issue facing volcanologists is to identify patterns in how these precursor signals change over time prior to an eruption, and discriminate the patterns that precede eruptions (i.e. arrival of lava at the surface) from those that precede failed eruptions (e.g. magma intrusion at shallow depths with no eruption), false alarms remaining a major challenge for volcano observatories and civil defense authorities. Improving our ability to predict when eruptions will begin has been highlighted by the community[5] and advances the above referenced Decadal Survey Theme.

Although much attention has been diverted to predicting when eruptions will begin, the 2010 eruption of Eyjafjallajökull, Iceland highlighted the need for accurate predictions of when an eruption will end, given the socio-economic disruption that results, and the problems that arise when governments cannot plan for eruptions of indeterminate length. During effusive, mafic, lava-flow forming eruptions, effusion rates typically increase rapidly to a peak, and then wane over a longer period of time until the eruption ends[10] (Fig. 6). Recent work[11] has demonstrated that satellite measurements of lava effusion rate, derived from long-wave infrared remote sensing measurements of the thermal emission from the lava flows erupted during mafic effusive eruptions, can be used to predict the end of lava effusion (and hence the eruption) to within <10% of the eruption duration itself. During these eruptions, and those that produce lava domes, gas emission rates also decrease as the supply of fresh magma from depth wanes[3]. Dome-forming eruptions may last years (Fig. 7), making long-term measurements of lava effusion and gas emission rates essential for recognizing changes that may be indicative of cessation of supply of fresh magma from depth. Determining how satellite measurements of effusion rate[12], degassing[13], and deformation[14] can be used to predict *the end* of an eruption is a high value science target.

APPLICATION TARGET: TO IMPROVE FORECASTS OF HAZARDS ASSOCIATED WITH TERRESTRIAL VOLCANISM, ONCE AN ERUPTION HAS BEGUN

Description of the application target, relevance to community needs and Decadal Survey Theme

Mitigating volcanic hazards to aviation: The hazards that volcanic ash clouds present to aviation are well documented[15]. During the 2010 eruption of Eyjafjallajökull (Fig. 8), Iceland, ash clouds grounded aircraft for eight days, costing airlines ~US$1.7 billion, with the cancellation of ~100,000 flights[16] affecting 10 million passengers. Remote sensing is the only feasible method for studying these cloud given their often huge areal extent and rapid temporal variation. Recent advances in ash transport and dispersion modeling have combined remote sensing estimates of mass concentration with models of the physico-chemical evolution of ash clouds[17] and meteorological models. Key challenges in the future will involve incorporating variations in ash composition, size, and shape into the estimates of mass loading, and validating ash retrievals, to predict the time-space evolution of ash clouds, and the concentration of ash at each point in space. In European airspace a new challenge for remote sensing will be to increase the sensitivity (and accuracy) of remote sensing measurements to low ash concentrations. Prior to Eyjafjallajökull aircraft were grounded if there was any ash present in the atmosphere. Post-Eyjafjallajökull, aircraft engine manufacturers stipulated an ash concentration of 2 mg/m^3 as a "safe" limit for engine operation[18], allowing aircraft to fly through airspace containing ash for the first time. A key target for the future is to establish how remote sensing methods can detect concentrations at this level, such that the remote measurements are precise enough to validate ash forecasting models.

Predicting how far lava flows will extend from the vent, and rate at which the flows advance: The June 2014 lava flow erupted at Kilauea volcano, Hawaii, extended 17 km within three months, extending to within 500 m of the town of Pahoa, resulting in months of uncertainty for residents.

The total cost of this small eruption was ~US$14.5 million, primarily for constructing emergency access roads. It is important to forecast which areas downslope are likely to be inundated by lava flows and their time-rate of advance. A key challenge is to predict these quantities for long-duration eruptions, where multiple flow units can advance during the same eruption, in response to changes in the mass flux driving flow propagation. Effusion rate is a key variable in parameterizing numerical lava flow simulations as it is the primary geophysical parameter (after chemical composition) that determines how far a lava flow can advance[19]. It has been shown how effusion rates can be estimated from remote sensing data[20,12], allowing remote sensing measurements of effusion rate to drive physics-based predictions of lava flow motion[21] (Fig. 9).

Predicting the temporal evolution of volcanic aerosol clouds: SO_2 gas emitted from volcanoes is converted to (respirable) H_2SO_4 aerosol as it moves from the vent[22]. The resulting plumes ("vog", or "volcanic smog") are harmful to animals, vegetation and humans as a result of acid deposition and respiration of the aerosol[23]. Atmospheric dispersion models exist (Fig. 10) that aim to predict how these vog clouds spread over populated areas[24]. However, these models rely on an estimate of the rate and efficiency (and how this varies with environmental conditions) at which the SO_2-to-H_2SO_4 conversion takes place, estimates that are presently poorly constrained[25]. Yet better predictions are required if health professionals are to monitor for its effects and target mediation efforts. Improved measurements of i) the amount of SO_2 emitted by persistently degassing volcanoes varies in space and time, and ii) how rapidly this is converted to aerosol, are of great importance to improving the value of these predictive models.

KEY GEOPHYSICAL VARIABLES THAT NEED TO BE MEASURED TO ADVANCE THESE SCIENCE AND APPLICATION TARGETS

Predicting when volcanic eruptions begin and end, and how the products they erupt (lava, ash, gas) spread in space and time requires a diverse set of geophysical measurements, which can be pursued using space-based techniques.

i) Ground deformation: deformation measurements are obviously a key variable. Measurements of surface displacements allow the source of the displacement (subsurface re-distribution of magma) to be resolved, including the depth, size, and shape of the magma body responsible[26,14].

ii) Gas emissions: composition and fluxes: SO_2 is the most commonly measured volcanic gas because of its low background concentrations in the atmosphere[27]. Measurements of the SO_2 flux (i.e. mass per time) can be integrated over time to yield the total amount of SO_2 emitted, and from this the volume of magma that arose to shallow crustal levels can be estimated[28], providing an independent estimate of subsurface magma volumes that that derived from deformation modelling. CO_2 is emitted in greater quantities than SO_2, exsolves at greater depth, and is relatively inert in shallow hydrothermal systems and the atmosphere[29,30]. This means that the flux of CO_2 from a volcano is a more direct function of that exsolved at depth, and given that this depth is greater an increase in CO_2 output can herald an increase in volcanic unrest before the subsequent shallow degassing of SO_2 (i.e. CO_2 may provide early warning).

iii) Low temperature thermal anomalies: temperature measurements of the surface of terrestrial volcanoes, for example fumarole fields, are key for identifying enhanced hydrothermal heating in response to shallow intrusion of magma[31].

iv) The color, temperature, and size of crater lakes: all three variables have been observed to vary prior to volcanic eruptions as rising magma increases the fluxes of energy and chemical elements into the water body[32,33,34].

v) Lava effusion rate: The mass flux of lava from a vent, during a felsic or mafic effusive eruption, is the most direct observation we have (when combined with knowledge of the surface deformation field and gas flux) of the pressure conditions within the magma reservoir, and can be used to estimate how magma erupted is partitioned between surface flows and hypabyssal intrusions[35,36]. Lava effusion rate, and how it varies during an eruption, is also crucial for forecasting lava flow lengths[19,21].

vi) Temperature and cooling rate of active lavas: The rate at which lava flows and dome cool controls changes in rheology that control their ability to flow[37], and are important data for lava flow simulations[38]. Changes in the surface thermal structure of lava domes can reflect pressurization and explosive potential[39].

vii) Spatio-temporal variations in the amount and concentration of ash in the atmosphere: During explosive eruptions the height to which ash is injected and the amount of ash are related to the mass eruption rate[40], which is difficult to estimate directly, but of great interest to volcanologists. Variations in the concentration of ash are of great relevance to aviation hazards.

viii) The spatio-temporal distribution of H_2SO_4 aerosol: measurements of the amount of aerosol emitted and how this varies in space and time during episodic eruptions, sustained eruptions, and non-eruptive degassing are required[41].

KEY REQUIREMENTS ON THE QUALITY AND COVERAGE OF THE MEASUREMENTS REQUIRED TO ACHIEVE THESE SCIENCE AND APPLICATION TARGETS

Volcanoes occur all over Earth's surface, do not turn off at night, and the aforementioned geophysical variables vary of all manner of time scales. As such, global, day-and-night mapping missions (not sampling missions) or multi-annual duration are required if global, multi-parametric remote sensing data sets with which changes in these geophysical signals can be resolved are to be acquired. This will allow the spatio-temporal variability of the aforementioned volcanogenic signals and processes to be quantified in a uniform manner, for many dozens of volcanoes at various stages of volcanic unrest, for which some will proceed to an eruption whereas others will not. A recent study[42] of 288 cases of volcanic activity between 2000 and 2011 has shed light on the time scales over which these signals can be expected to occur prior to eruption, ranging from two days for complex volcanoes, one month for stratovolcanoes, two months at large calderas, and four months for shield volcanoes. Multi-temporal measurements of the co-variance of these key precursory volcanic variables, at a temporal resolution required to sample these characteristic pre-eruption unrest periods (i.e. sub-weekly), across multi-annual time scales, will allow the changes that take place as volcanoes enter periods of heightened unrest to be determined. Phillipson et al.[42]

found that the duration of non-eruptive unrest increased to <two months at stratovolcanoes, with a median duration of >6 months at calderas and shield volcanoes. Such a dense temporal sample, at the global scale would also provide immensely useful for the growing number of models that seek to predict volcanic behavior and hazards (deterministic and stochastic) that require large volumes of data regarding degassing, ground deformation, and lava effusion rate to run[43,44,45,21].

Previously, volcanologists have leveraged low spatial resolution (e.g. >1 km IFOV) remote sensing instruments (MODIS, AVHRR, GOES, OMI, AIRS, TOMS) because the high temporal resolution required to study dynamic volcanic phenomena was deemed to be more important than the lack of sensitivity (e.g. to low temperature thermal anomalies, or diffuse gas plumes)[46-53]. Yet many studies have shown how the higher sensitivity afforded by high spatial resolution (i.e. ≤100 m IFOV) but low temporal resolution/sampling missions (such as Terra ASTER, EO-1 Hyperion, and Landsat) markedly improves the fidelity with which the key geophysical parameters can be retrieved[54-63]. A high resolution (≤100 m IFOV), global mapping, day-night, high temporal resolution (sub-weekly) observation capability would greatly enhance the role that space-based observations can play in tackling the stated science and application targets.

Regarding spectral sampling, quantifying the aforementioned ensemble of key geophysical variables require measurements between visible to short-wave infrared (0.4-2.5 μm; lava flow temperature, volcanic aerosols, hydrothermal alteration, crater lake color), mid-wave infrared (3-5 μm; active lava detection), long-wave infrared (8-14 μm; SO_2, volcanic ash) and microwave (deformation) wavelengths, and much is to be gained from an observation strategy that acquires data at all of these wavelengths (near) simultaneously at the spatial and temporal resolutions discussed above. Several studies have shown the advantages of hyperspectral data at VSWIR and TIR wavelength for quantifying these variables at high spatial resolution[58,60,64-67], and imaging spectrometers will be a vital component of future volcano observation systems. For example, recent work has shown how VSWIR imaging spectrometers can quantify atmospheric CO_2 from point sources, including volcanoes[68,69]. Such a capability would be of great value to the volcanological community.

LIKELIHOOD OF AFFORDABLY ACHIEVING THE REQUIRED MEASUREMENTS

Several InSAR missions are already in development and will combine to yield the required deformation data. The imaging approaches and technologies required to provide volcanologists with the high spatial resolution VSWIR-MWIR-TIR data required are in comparison inexpensive and much work has been done developing the relevant technologies. The Decadal Survey HyspIRI mission, for example, was priced at ~$600M. The proliferation of small, micro, and even cube satellites will further increase the likelihood that these measurements can be made. For example, Blue Canyon Technologies offer a 6U cube-sat, with X-band telemetry, for $600K (bluecanyontech.com). Spaceflight currently quote $545K for a 6U CubeSat launch (www.spaceflight.com).

CITATIONS

1. Doocy, S., Daniels, A., Dooling, S., and Gorokhovich, Y. (2013). The Human Impact of Volcanoes: a Historical Review of Events 1900-2009 and Systematic Literature Review. *PLOS Currents Disasters*. doi: 10.1371/currents.dis.841859091a706efebf8a30f4ed7a1901.

2. Aspinall, W.et al., (2011). Bristol University Cabot Institute and NGI Norway for the World Bank, *NGI Report 20100806*, 3.

3. Sparks, R.S.J., Biggs, J., and Neuberg, J.W. (2012). Monitoring volcanoes. *Science*, 335, 1310-1311.

4. Moran, S.C., Freymueller, J.T., LaHusen, R.G., McGee, K.A., Poland, M.P., Power, J.A., Schmidt, D.A., Schneider, D.J., Stephens, G., Werner, C.A., White, R.A., (2008). Instrumentation Recommendations for Volcano Monitoring at U.S. Volcanoes Under the National Volcano Early Warning System. *U.S. Geological Survey Scientific Investigations Report*, 2008–5114, 47 p.

5. Davis, J. L., L. H. Kellogg, J. R. Arrowsmith, B. A. Buffett, C. G. Constable, A., Donnellan, E. R. Ivins, G. S. Mattioli, S. E. Owen, M. E. Pritchard, M. E. Purucker, D. T. Sandwell, and J. Sauber (2016), Challenges and Opportunities for Research in ESI (CORE): Report from the NASA Earth Surface and Interior (ESI) Focus Area Workshop, November 2–3, 2015, Arlington, Virginia, xx pp., doi: TBD.

6. Wohletz, K., and Heiken, G. (1992). Volcanology and geothermal energy. Los Angeles, University of California Press.

7. Pasternack, G.B., and Varekamp, J.C. (1997). Volcanic lake systematics I. Physical constraints. *Bull. Volcanol.*, 58, 528–538.

8. Badrudin, M. (1994). Kelut volcano monitoring: hazards, mitigation and changes in water chemistry prior to the 1990 eruption. *Geochem. J.,* 28, 233–241.

9. Gottsmann, J. (2015) Volcanic unrest and short-term forecasting capacity. In: S.C. Loughlin, R.S.J. Sparks, S.K. Brown, S.F. Jenkins and C. Vye-Brown (Eds.), *Global Volcanic Hazards and Risk*, Cambridge: Cambridge University Press.

10. Wadge, G. (1981). The variation of magma discharge during basaltic eruptions. *J. Volcanol. Geotherm. Res.*, 11, 139–168.

11. Bonny, E., and Wright, R. (2015). Predicting the End of Lava-Flow-Forming Eruptions from Space, V24B-04, presented at 2015 Fall Meeting, AGU, San Francisco, Calif., 14-19 Dec.

12. Wright, R., Blake, S., Harris, A.J.L., and Rothery, D.A., (2001). A simple explanation for the space-based calculation of lava eruption rates. *Earth Planet. Sci. Lett*., 192, 223–233.

13. Realmuto, V.J. (2000). The potential use of Earth Observing System data to monitor the passive emission of sulphur dioxide from volcanoes. In P. Mouginis-Mark, J. Crisp, and J. Fink (Eds.), *Remote Sensing of Active Volcanism*, AGU Monograph 116, American Geophysical Union, Washington D.C., p. 101-115.

14. Lu, Z., and Dzurisin, D. (2014). InSAR imaging of Aleutian volcanoes: monitoring a volcanic arc from space. Heidelberg, Springer Praxis Books.

15. Webley, P., and Mastin, L. (2009). Improved prediction and tracking of volcanic ash clouds. *J. Volcanol. Geotherm. Res.*, 186, 1–9.

16. Anonymous. (2011, April 14). Eyjafjallajokull one year on: the fire next time. *The Economist*.

17. Corradini, S., Merucci, L., and Folch, A. (2011). Volcanic Ash Cloud Properties: Comparison Between MODIS Satellite Retrievals and FALL3D Transport Model. *IEEE Geosci. Remote Sens. Lett*., 8, 248-252.

18. Kueppers, U., Cimarelli, C., K-U, Hess, Taddeucci, J., Wadsworth, F.B., Dingwell, D.B., (2014). The thermal stability of Eyjafjallajökull ash versus turbine ingestion test sands. J. App. Volcanol., 3, 3:4.

19. Walker, G.P.L., (1973). Lengths of lava flows. *Phil. Trans. Royal Soc. Lond*., 273, 107–118.

20. Harris, A.J.L., Blake, S., Rothery, D.A., and Stevens, N.F. (1997). A chronology of the 1991 to 1993 Etna eruption using advanced very high resolution radiometer data: implications for real–time thermal volcano monitoring. *J. Geophys. Res*., 102, 7985–8003.

21. Wright, R., Garbeil, H., and Harris, A.J.L. (2008). Using infrared satellite data to drive a thermo-rheological/stochastic lava flow emplacement model: a method for near-real-time volcanic hazard assessment. *Geophys. Res. Lett*., 35, L19307, doi:10.1029/2008GL035228.

22. Sutton, A. J., and Elias, T. (1993). Volcanic gases create air pollution on the island of Hawai‘i. *Earthquakes and Volcanoes*, Vol. 24, U.S. Geological Survey, Reston, VA, 178–196.

23. Williams-Jones, G. and Rymer, H. (2000) Hazards of Volcanic Gases. In H. Sigurdsson, B. Houghton, H. Rymer, J. Stix, S. McNutt (Eds.), *Encyclopedia of Volcanoes*, Academic Press, 997-1004.

24. Businger, S., Huff, R., Pattantyus, A., Horton, K., Sutton, A.J., Elias, T., and Cherubini, T., (2015). Observing and forecasting vog dispersion from Kilauea volcano, Hawaii. *Bull. Amer. Meteor. Soc.*, 96, 1667-1686.

25. Textor, C., Graf, H.-F., Timmreck, C., and Robock, A. (2004). Emissions from volcanoes. In: C. Granier, P. Artaxo, and C.E. Reeves (Eds.), *Emissions of atmospheric trace compounds*. Kluwer Academic Publishers, pp. 269-303.

26. Segall, P. (2010). *Earthquake and Volcano Deformation*, Princeton University Press.

27. Seinfeld, J. H. and Pandis, S. N. (1997). *Atmospheric chemistry and physics*. New York, John Wiley and Sons.

28. Sutton, A.J., Elias, T., and Kauahikaua, J., (2003). Lava-effusion rates for the Pu‘u ‘Ō‘ō–Kūpaianaha eruption derived from SO_2. In: Heliker C, Swanson DA, Takahashi TJ (eds) *The Pu‘u ‘Ō‘ō–Kūpaianaha eruption of Kīlauea volcano, Hawai‘i: the first 20 years*. USGS Professional Paper 1676, pp 137–148.

29. Burton, M.R., Oppenheimer, C., Horrocks, L.A., and Francis, P.W. (2000). Remote sensing of CO_2 and H_2O emissions from Masaya volcano, Nicaragua. *Geology*, 28, 915-918.

30. Edmonds, M. (2008). New geochemical insights into volcanic degassing. *Philos. Trans. R. Soc. Lond*., A, 366, 4559-4579.

31. Italiano, F., Pecoraino, G., and Nuccio, P.M., (1998). Steam output from fumaroles of an active volcano: Tectonic and magmatic-hydrothermal controls on the degassing system at Vulcano (Aeolian arc). *J. Geophys. Res*., 103, 29,829-29,842.

32. Moore, J.G., Nakamura, K., and Alcarez, A. (1966). The eruption of Taal volcano, Philippines, September 28-30, 1965. *Science*, 151, 955–960.

33. Christenson, B.W. (1994). Convection and stratification in Ruapehu crater lake, New Zealand: implications for Lake Nyos–type gas release eruptions. *Geochem. J*., 28, 185–197.

34. Brown, G., Rymer, H., Dowden, J., Kapadia, P., Stevenson, D., Barquero, J., and Morales, L.D. (1989). Energy budget analysis for Poas crater lake: implications for predicting volcanic activity. *Nature*, 339, 370–373.

35. Steffke, A.M., Harris. A.J.L., Burton, M., Caltabiano, T., and Salerno, G. (2011). Coupled use of COSPEC and satellite measurements to define the volumetric balance during effusive eruptions at Mt. Etna, Italy. *J. Volcanol. Geotherm. Res*. 205, 47-53.

36. Koeppen, W.C., Patrick, M., Orr, T., Sutton, J., Dow, D., and Wright, R. (2013). Constraints on the partitioning of Kilauea's lavas between surface and tubed flows, estimated from infrared satellite data, sulfur dioxide flux measurements, and field observations. *Bull. Volcanol*., 75, doi:10.1007/s00445-013-0716-3.

37. Harris, A.J.L., Bailey, J., Calvari, S., and Dehn, J., (2005). Heat loss measured at a lava channel and its implications for down-channel cooling rheology, in: Mangan, M., Ventura, G., (Eds.) *Kinematics and dynamics of lava flows*. Boulder, Colo.: Geological Society of America., pp 125–146.

38. Harris, A.J.L., and Rowland, S.K., (2001). FLOWGO: a kinematic thermo-rheological model for lava flowing in a channel. *Bull. Volcanol*., 63, 20-44.

39. Matthews, S. J., Gardeweg, M. C. and Sparks, R. S. J. (1997). The 1984 to 1996 cyclic activity of Lascar Volcano, northern Chile: Cycles of dome growth, dome subsidence, and explosive eruptions. *Bull. Volcanol*. 59, 77-82.

40. Ripepe, M., Bonadonna, C., Folch, A., Delle Donne, D., Lacanna, G., Marchetti, E., and Hoskuldsson, A., (2013). Ash-plume dynamics and eruption source parameters by infrasound and thermal imagery: The 2010 Eyjafjallajokull eruption. *Earth Planet. Sci. Lett*., 366, 112-121.

41. Mather, T.M., Pyle, D.M, and Oppenheimer, C. (2003). Tropospheric volcanic aerosol, in A. Robock and C. Oppenheimer, (Eds.), *Volcanism and Earth's Atmosphere*, AGU Monograph 139, American Geophysical Union, Washington D.C., p. 189-212.

42. Phillipson, G., Sobradelo, R., and Gottsmann, J. (2013). Global volcanic unrest in the 21st century: an analysis of the first decade. *J. Volcanol. Geotherm. Res.*, 264, 183–196.

43. Anderson, K., and Segall, P. (2011). Physics-based models of ground deformation and extrusion rate at effusively erupting volcanoes, *J. Geophys. Res*., 116, DOI: 10.1029/2010JB007939.

44. Passarelli, L., Sansò, B., Sandri, L., Marzocchi. W. (2010). Testing forecasts of a new Bayesian time-predictable model of eruption occurrence. *J. Volcanol. Geotherm. Res.*, 118, 57–75.

45. Vitturi, M.M., Neri, A., and Barsotti, S. (2015). PLUME-MoM 1.0: A new integral model of volcanic plumes based on the method of moments. *Geosci. Model Dev.,* 8, 2447-2463.

46. Harris, A.J.L., Blake, S., Rothery, D.A., and Stevens, N.F. (1997). A chronology of the 1991 to 1993 Etna eruption using advanced very high resolution radiometer data: implications for real–time thermal volcano monitoring. *J. Geophys. Res*., 102, 7985–8003.

47. Wright, R., De La Cruz-Reyna, S., Harris, A.J.L., Flynn, L.P., and Gomez-Palacios, J.J., (2002). Infrared satellite monitoring at Popocatepetl: explosions, exhalations, and cycles of dome growth. *J. Geophys. Res.,* 107, 10.1029/2000JB000125.

48. Carn, S. A., Krueger, A.J., Bluth, G., Schaefer, S.J., Krotkov, N.A., Watson, I.M., and Datta, S. (2003). Volcanic eruption detection by the Total Ozone Mapping Spectrometer (TOMS)

instruments: a 22-year record of sulphur dioxide and ash emissions In: Oppenheimer et al. (Eds) *Volcanic Degassing*. London, Geological Society of London. p. 177-202.

49. Filizzola, C., Lacava, T., Marchese, F., Pergola, N., Scaffidi, I., and Tramutoli, V. (2007). Assessing RAT (Robust AVHRR Techniques) performances for volcanic ash cloud detection and monitoring in near real-time: the 2002 eruption of Mount Etna (Italy). *Remote Sens. Environ*., 107, 440-454.

50. Novak, M.A.M., Watson, I.M., Delgado-Granados, H., Rose, W.I., Cardenas-Gonzalez, L., and Realmuto, V.J . (2008). Volcanic emissions from Popocatepetl volcano, Mexico, quantified using moderate resolution imaging spectroradiometer (MODIS) infrared data: A case study of the December 2000–January 2001 emissions. *J. Volcanol. Geotherm. Res*., 170, 76–85.

51. Prata, A.J., and Bernardo, C., (2007). Retrieval of volcanic SO_2 column abundance from Atmospheric Infrared Sounder data. *J. Geophys. Res*., 112, doi:10.1029/2006JD007955.

52. van Manen, S., Blake, S., Dehn, J., and Valcic, L. (2013). Forecasting large explosions at Bezymianny Volcano using thermal satellite data. *Geol. Soc. Lond. Spec. Pub*. 380, 187-201.

53. Wright, R., Flynn, L.P., Garbeil, H., Harris, A.J.L., and Pilger, E. (2002). Automated volcanic eruption detection using MODIS. *Remote Sens. Environ*., 82, 135–155.

54. Pieri, D., and Abrams, M. (2005). ASTER observations of thermal anomalies preceding the April 2003 eruption of Chikurachki volcano, Kurile Islands, Russia. *Remote Sensing Environ*., 99, 84-94.

55. Urai, M., (2004). Sulfur dioxide flux estimation from volcanoes using Advanced Spaceborne Thermal Emission and Reflection Radiometer – a case study of the Miyakejima volcano, Japan. *J. Volcanol. Geotherm. Res*., 134, 1–13.

56. Pugnaghi, S., Gangale, G., Corradini, S., and Buongiorno, M.F., (2006). Mt. Etna sulfur dioxide flux monitoring using ASTER–TIR data and atmospheric observations, *J. Volcanol. Geotherm. Res*., 152, 74–90.

57. Trunk, L., and Bernard, A. (2008). Investigating crater lake warming using ASTER thermal imagery: Case studies at Ruapehu, Poás, Kawah Ijen, and Copahué Volcanoes. *J. Volcanol. Geotherm. Res*. 178, 259-270.

58. Wright, R., H. Garbeil, and Davies, A.G., (2010). Cooling rate of some active lavas determined using an orbital imaging spectrometer. *J. Geophys. Res.,* 115, B06205, doi:10.1029/2009JB006536.

59. Ramsey, M.S., and Fink, J. H. (1999). Estimating silicic lava vesicularity with thermal remote sensing: a new technique for volcanic mapping and monitoring. *Bull. Volcanol.*, 61, 32-39.

60. Wright, R., Glaze, L., and Baloga, S.M., (2011). Constraints on determining the eruption style and composition of terrestrial lavas from space. *Geology*, 39, 1127-1130.

61. Vaughan, R.G., Keszthelyi, L.P., Lowenstern, J.B., Jaworowski, C., Heasler, H. (2012). Use of ASTER and MODIS thermal infrared data to quantify heat flow and hydrothermal change at Yellowstone National Park. *J. Volcanol. Geotherm. Res*. 233-234, 72-89.

62. Oppenheimer, C., Francis, P.W., Rothery, D.A., Carlton, R.W.T., and Glaze, L.S., (1993). Infrared image analysis of volcanic thermal features: Lascar Volcano, Chile, 1984–1992. *J. Geophys. Res.*, 98, 4269–4286.

63. Harris, A.J.L., Flynn, L.P., Rothery, D.A., Oppenheimer, C., and Sherman, S.B., (1999). Mass flux measurements at active lava lakes: implications for magma recycling. *J. Geophys. Res*., 104, 7117–7136.

64. Spinetti, C., Buongiorno, M.F., Lombardo, V., and Merucci, L., (2003). Aerosol optical thickness of Mt. Etna volcanic plume retrieved by means of the Airborne Multispectral Imaging Spectrometer (MIVIS). *Ann. Geophys*., 46, 439-449.

65. Crowley, J.K., Hubbard, B.E., and Mars, J.C. (2003). Analysis of potential debris flow source areas on Mount Shasta, California, by using airborne and satellite remote sensing data. *Remote Sens. Environ*., 87, 345-358.

66. Lombardo, V., Harris, A.J.L., Calvari, S., and Buongiorno, M.F., (2009). Spatial variations in lava flow field thermal structure and effusion rate derived from very high spatial resolution hyperspectral (MIVIS) data. *J. Geophys. Res*., 114, DOI: 10.1029/2008JB005648.

67. Gabrieli, A., Wright, R., Lucey, P.G., Garbeil, H., Pilger, E., Porter, J.N., and Wood, M. (2016). Characterization and initial field test of a long wave infrared thermal hyperspectral imager for measuring SO_2 in volcanic plumes. *Bull. Volcanol*., sub. judice.

68. Dennison, P.E., A.K. Thorpe, E.R. Pardyjak, D.A. Roberts, Y. Qi, R.O. Green, E.S. Bradley, and C.C. Funk, 2013. High spatial resolution mapping of elevated atmospheric carbon dioxide using airborne imaging spectroscopy: Radiative transfer modeling and power plant plume detection. *Remote Sensing Environ*., 139, 116-129.

69. Spinetti, C., Carrere, V., Buongiorno, M.F., Sutton, A.J., Elias, T., (2008). Carbon dioxide of Pu`u`O`o volcanic plume at Kilauea retrieved by AVIRIS hyperspectral data. *Remote Sensing Environ*., 112, 3192-3199.

FIGURES

Figure 1. Distribution of Earth's active and potentially active volcanoes (source: Sigurdsson, H. (2015). *Encyclopedia of volcanoes*, 2nd edition. San Diego: Academic Press.

Figure 2. Deformation of Peulik volcano, Alaska, over a two year period, derived from the satellite-based InSAR technique (source: Lu, Z., and Dzurisin, D. (2014). *InSAR imaging of Aleutian volcanoes: monitoring a volcanic arc from space*. Heidelberg, Springer Praxis Books).

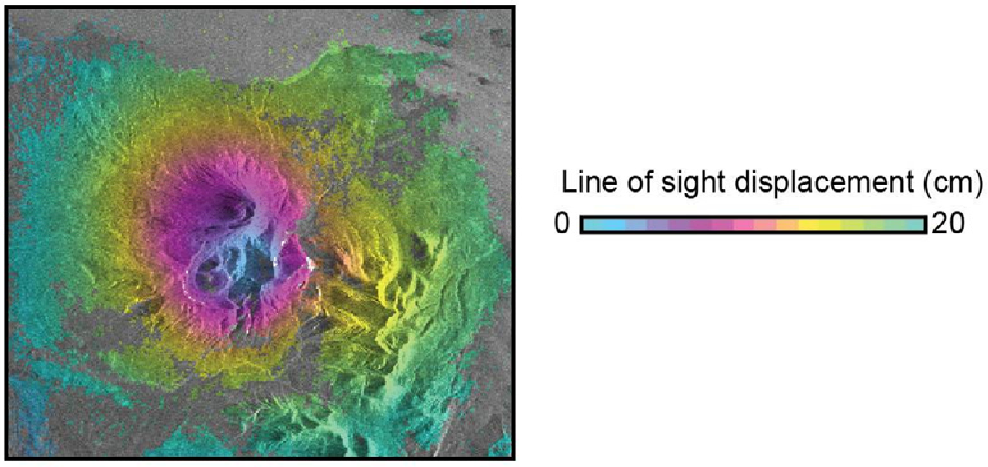

Figure 3. SO_2 column abundance calculated from Terra ASTER data at Kilauea volcano (source: https://hyspiri.jpl.nasa.gov/downloads/2013_Workshop/day1/18_HyspIRI_VJR_2013.pdf)

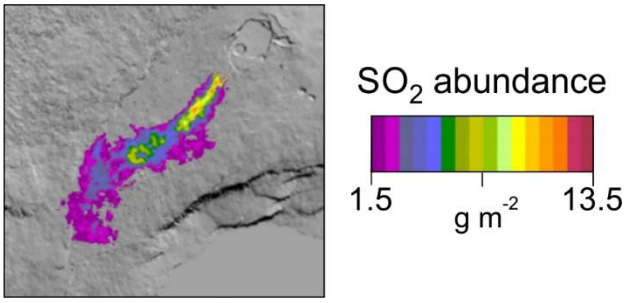

Figure 4. Left: Landsat ETM+ true color composites of the crater lakes at Maly Semyachik, Russia (left) and Irazu (Costa Rica, right) with corresponding photographs beneath (source: Wright, R. (2015). Remote sensing of volcanoes. In: P. Thenkabail (Ed.) *The Remote Sensing Handbook*, Volume III, CRC Press, p. 515-544.). Right. ASTER-derived crater lake temperatures at Mount Ruapehu, New Zealand. Open triangles are in-situ data, filled circles are ASTER measurements (source: Trunk, L., and Bernard, A. (2008). Investigating crater lake warming using ASTER thermal imagery: Case studies at Ruapehu, Poás, Kawah Ijen, and Copahué Volcanoes. *J. Volcanol. Geotherm. Res*. 178, 259-270.)

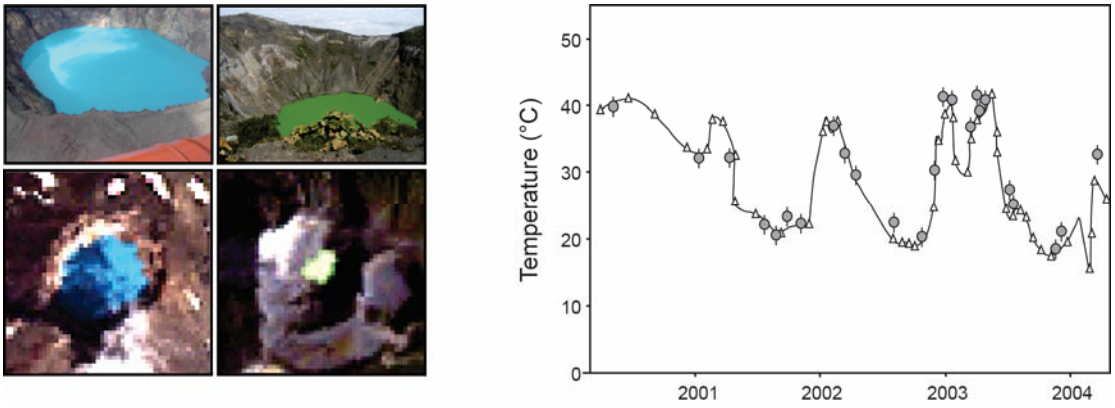

Figure 5. Left: Reflective false color composite of Chiliques Volcano, Chile, obtained by Terra ASTER. Right: thermal infrared night-time image of the same volcano showing subtle thermal anomaly at the summit (source: Pieri, D.C., and Abrams, M. (2004). ASTER watches the world's volcanoes: a new paradigm for volcanological observations from orbit. *J. Volcanol. Geotherm. Res.*, 135, 13-28).

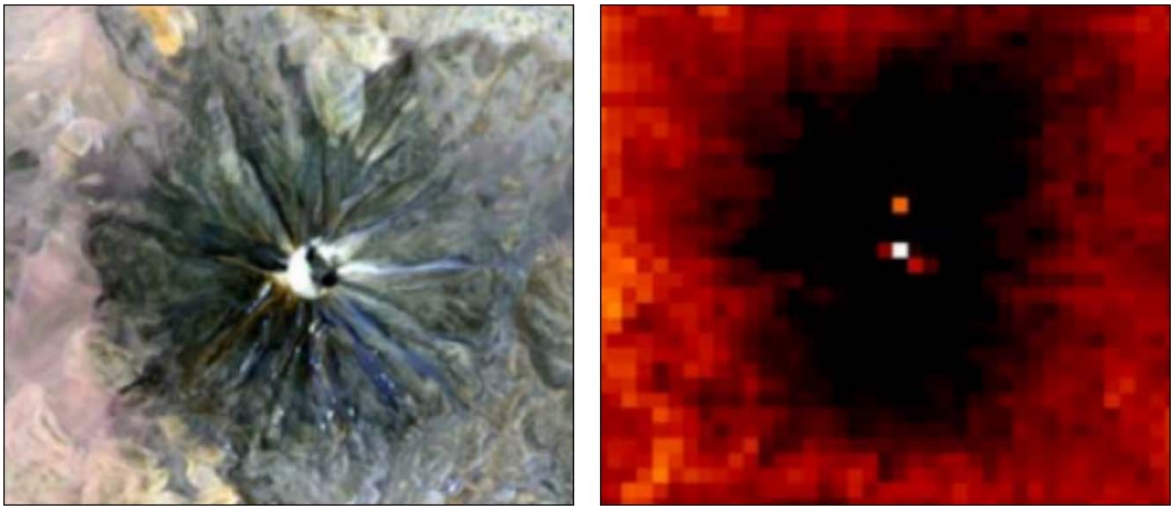

Figure 6. Lava effusion rates estimated using Terra and Aqua MODIS data (red line) during the 2014-2015 eruption of Holohraun, Iceland. Ground based estimates shown in blur triangles (source: Bonny, E., Thordarsson, T., and Wright, R. (2016). The volume of lava erupted during the 2014 to 2015 eruption of Holuhraun, Iceland: a comparison between satellite- and ground-based measurements. *Geophys. Res. Lett*., in review).

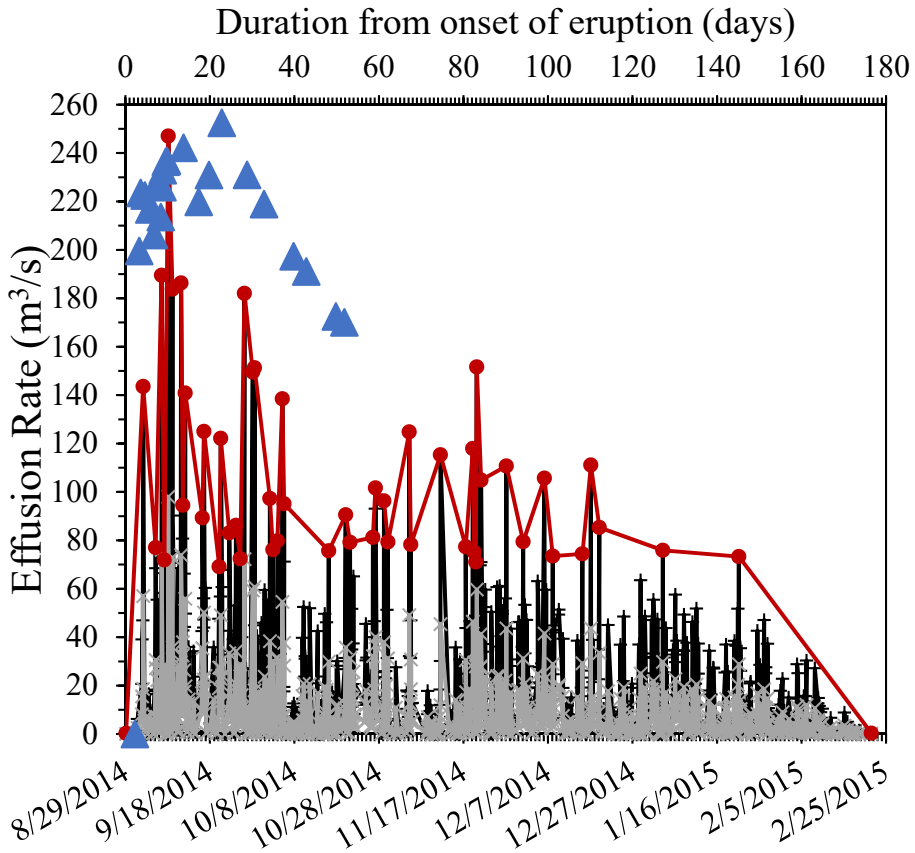

Figure 7. Energy radiated by the Soufriere Hills Volcano lava dome during the 1995-2011 eruption (source: Wright, R. (2015). MODVOLC: 14 years of autonomous observations of effusive volcanism from space. In: A. Harris, T. DeGroove, F. Garel, and S. Carn, (Eds.), *Detecting, modelling, and responding to effusive eruptions*. Special Publication of the Geological Society of London, 426, doi:10.1144/SP426.12.)

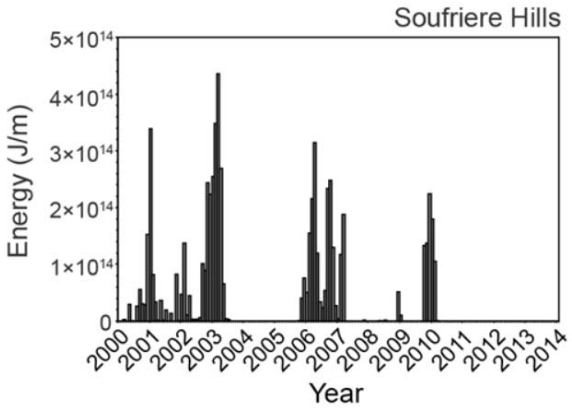

Figure 8. Left: Terra MODIS simulated true color composite (bands 1, 4, and 3 in red, green, and blue) of the ash cloud produced during the 2010 eruption of Eyjafjallajökull, Iceland. The ash cloud is clearly visible as the brown streak running approximately north-south. Center: MODIS band 31 (11.02 μm) minus MODIS band 32 (12.02 μm) brightness temperature difference (BTD) image. The black pixels running north-south correspond to strongly negative BTD values. Right: three BTD profiles across the image subset (red lines mark transects). The horizontal scale is the same as for the horizontal transect on the images displayed (source: Wright, R. (2015). Remote sensing of volcanoes. In: P. Thenkabail (Ed.) *The Remote Sensing Handbook*, Volume III, CRC Press, p. 515-544.)

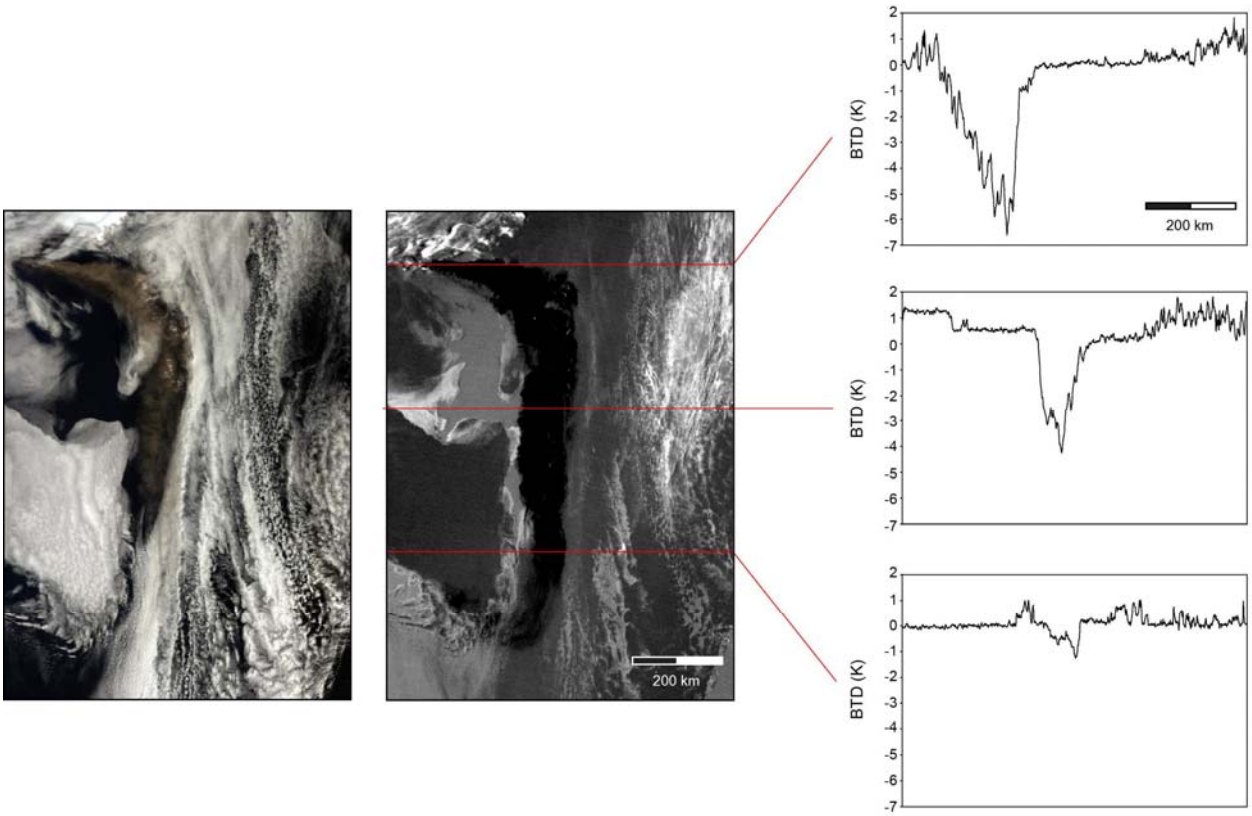

Figure 9. Lava flow simulations derived using infrared remote sensing-derived lava effusion rates at four dates during the 1991-1993 eruption of Mount Etna, Sicily. Black line diagrams beneath show the actual dimensions of the flow, as obtained from field observations, at each time (source: Wright, R., Garbeil, H., and Harris, A.J.L. (2008). Using infrared satellite data to drive a thermo-rheological/stochastic lava flow emplacement model: a method for near-real-time volcanic hazard assessment. *Geophys. Res. Lett*., 35, L19307, doi:10.1029/2008GL035228.).

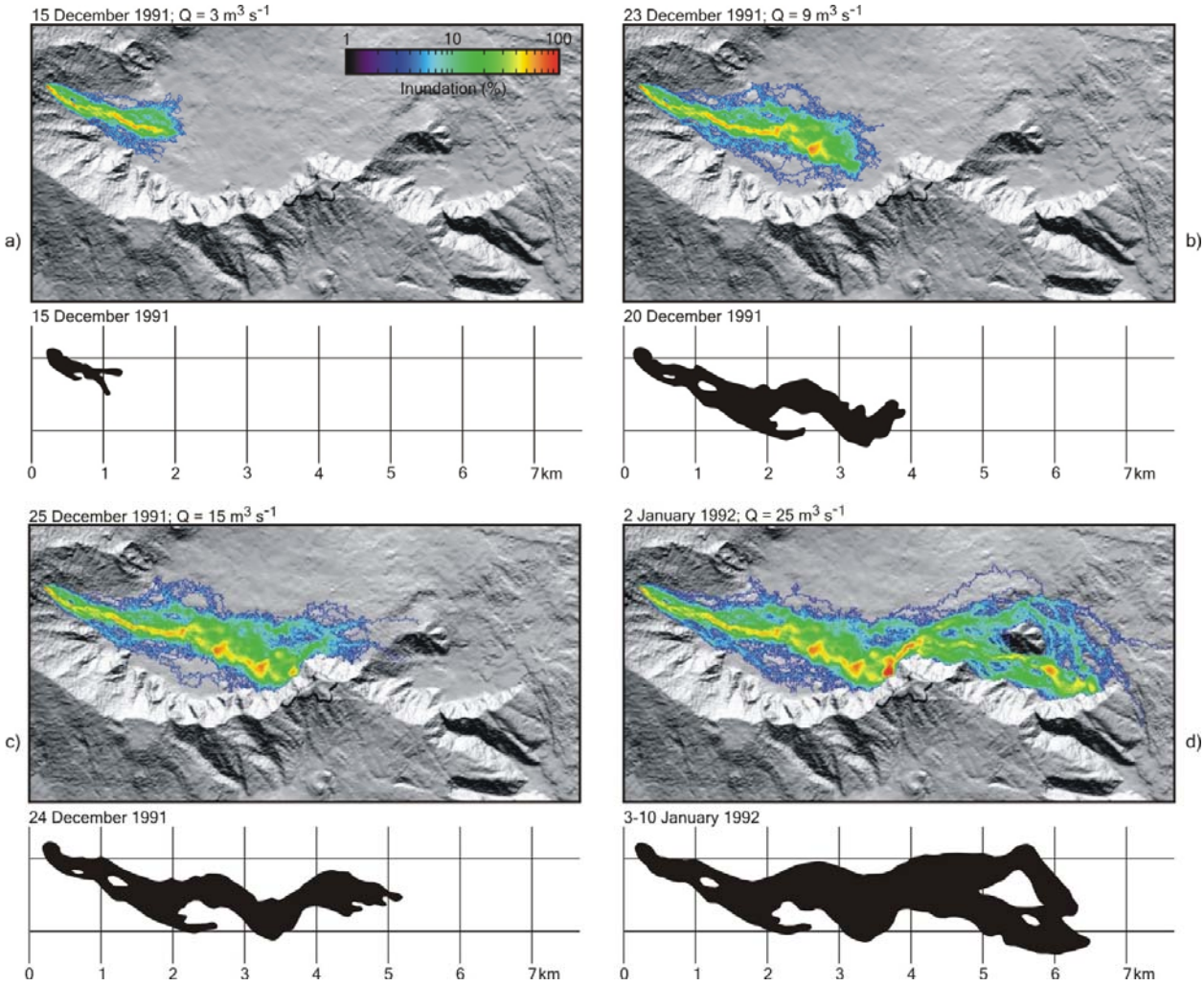

Figure 10. Top: OMI-derived SO_2 column abundances at in the State of Hawaii. Bottom: modelled ground-level H_2SO_4 concentrations (source: Businger, S., Huff, R., Pattantyus, A., Horton, K., Sutton, A.J., Elias, T., and Cherubini, T., (2015). Observing and forecasting vog dispersion from Kilauea volcano, Hawaii. *Bull. Amer. Meteor. Soc.*, 96, 1667-1686.)